Magnetic phase diagrams of the manganites $Ln_{1-x}Ba_xMnO_3$ (Ln = Nd, Sm)

1999 J. Phys.: Condens. Matter 11 8707

(http://iopscience.iop.org/0953-8984/11/44/309)

J. Phys.: Condens. Matter **11** (1999) 8707–8717. Printed in the UK PII: S0953-8984(99)03694-2

Magnetic phase diagrams of the manganites $Ln_{1-x}Ba_xMnO_3$ (Ln = Nd, Sm)

I O Troyanchuk†, D D Khalyavin†, S V Trukhanov† and H Szymczak‡

† Institute of Physics of Solids and Semiconductors, National Academy of Sciences, P Brovki Street 17, 220072 Minsk, Belarus

‡ Institute of Physics of Academy of Sciences, Al. Lotniko'w 32/46, 02-668 Warsaw, Poland

Received 23 April 1999, in final form 28 June 1999

Abstract. The magnetization and magnetoresistance of $Ln_{1-x}Ba_xMnO_3$ have been studied for a single crystal (Ln = Nd, $x = 0.23$) and for ceramics (Ln = Nd, Sm; $0 \leqslant x \leqslant 0.44$). It was shown that $Nd_{1-x}Ba_xMnO_3$ compositions in the range $0 \leqslant x \leqslant 0.05$ are inhomogeneous antiferromagnets; a mixed antiferro–ferromagnet state appears in the range $0.05 < x < 0.10$; a pure ferromagnetic state develops in the range $0.2 \leqslant x < 0.4$ and in the range $x \geqslant 0.4$ an inhomogeneous ferromagnetic state is realized. Metal-like behaviour below T_C is found in the concentration $0.3 < x \leqslant 0.44$. The concentrational transition from inhomogeneous antiferromagnetic state into spin-glass state in $Sm_{1-x}Ba_xMnO_3$ was found at $x > 0.12$. Both Nd and Sm sublattices are coupled antiferromagnetically with manganese ions. All the ferromagnetic $Nd_{1-x}Ba_xMnO_3$ samples show similar magnetotransport properties despite of a strong difference in the resistivity behaviour. Our results could be understood in terms of Mn–O–Mn superexchange and 3d orbital ordering as well as variation of band structure due to the ionic size effect, Mn^{4+} ion appearance and magnetic ordering. It is supposed that the gap between the narrow 3d manganese band and wide 2p oxygen band decreases strongly below T_C.

1. Introduction

Among the various manganese perovskites which have been explored only the manganites $Ln_{1-x}Ba_xMnO_3$ exhibit very small crystal structure distortions in a wide range of the lanthanide ionic radii [1–5]. The magnetic and magnetoresistance properties of $Ln_{2/3}Ba_{1/3}MnO_3$ (Ln = La, Pr, Nd) are similar in many aspects: these almost cubic perovskites show a metal–insulator transition and peak of the magnetoresistance near their T_C [2]. However $Ln_{2/3}Ba_{1/3}MnO_3$ (Ln = Sm, Eu, Gd) show spin-glass-like behaviour despite very small crystal structure distortions and close unit cell volume in comparison with the ferromagnetic $Nd_{2/3}Sr_{1/3}MnO_3$ composition [2]. In another respect the Ba-doped manganites should be of interest due to the high mismatch between lanthanide and Ba ionic size. Recently it has been suggested that the difference between lanthanide and alkaline earth ionic radii reduces strongly the T_C value by favouring the formation of Jahn–Teller distortions [6]. The magnetic and magnetotransport properties of $Ln_{1-x}Ba_xMnO_3$ (Ln = Nd, Sm) series as a function of barium concentration and oxygen content have not been studied yet. In the present work we are reporting the comparative investigation of these systems undertaken for better understanding of the magnetic and magnetotransport properties of the manganites near the concentrational phase transition.

0953-8984/99/448707+11$30.00

2. Experiment

The single crystals of $Nd_{0.77}Ba_{0.23}MnO_3$ composition were received from B_2O_3-BaO-BaF_2 flux by slow cooling in air from 1150 °C in a platinum crucible. Nearly cubic crystals with edges ranging from 2 to 5 mm were selected for magnetic and magnetotransport measurements. We could not obtain good quality Sm-based single crystals in spite of the wide range of synthesis conditions.

The polycrystalline samples were prepared by mixing $BaCO_3$, Nd_2O_3 or Sm_2O_3 and Mn_2O_3 in the desired proportion. After prefiring at 900 °C the mixtures were pressed in the form of discs and sintered at 1470 °C for 4 r. All the samples were cooled slowly with a furnace at a rate of 80 °C h^{-1}. According to our x-ray data, the samples in the range $0 \leqslant x \leqslant 0.44$ were single phase whereas in some cases for $x = 0.5$ a small amount of foreign phases (below 5%) was detected. We think that the upper limit of barium substitution for the samples prepared in air is slightly below the $x = 0.5$ composition. Some of the samples prepared in air were reduced in vacuum at 800 °C using silica tubes and metallic tantalum as getter. The oxygen content for selected samples was determined by a thermogravimetric analysis.

Magnetization measurements were carried out using a commercial vibrating sample magnetometer. The electrical resistance measurements were performed by a standard four probe method using ultrasonically deposited indium contacts.

3. Results and discussion

The unit cell parameters are listed in table 1. $Nd_{1-x}Ba_xMnO_3$ in the concentration range $0 < x < 0.1$ exhibit the large so-called O′-orthorhombic distortions which, according to [7], could be attributed to the cooperative Jahn–Teller effect. In the samples with barium content above $x = 0.1$ Jahn–Teller distortions are removed; however the unit cell remains orthorhombically distorted ($c/a\sqrt{2} > 1$). These distortions arise from mismatch between

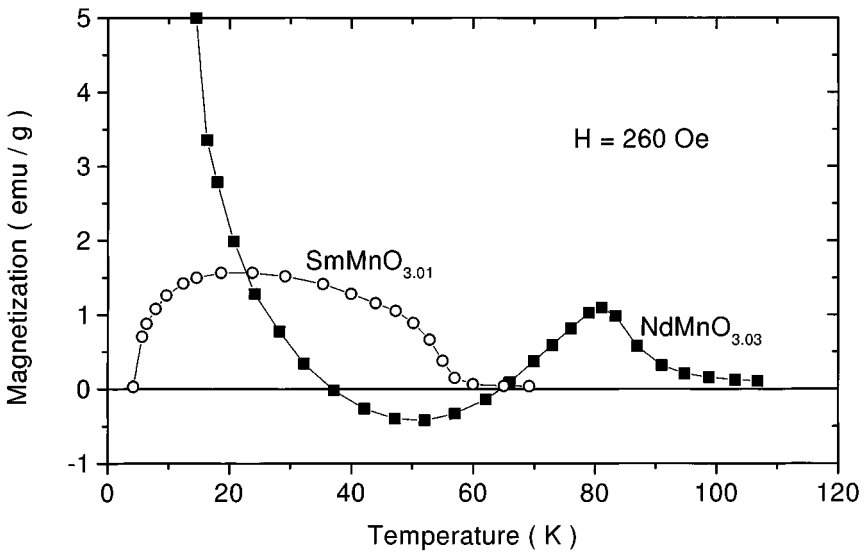

Figure 1. Magnetization as a function of temperature for the $NdMnO_{3.03}$ and $SmMnO_{3.01}$ compounds registered in a field of 260 Oe after cooling in a field of 11 kOe.

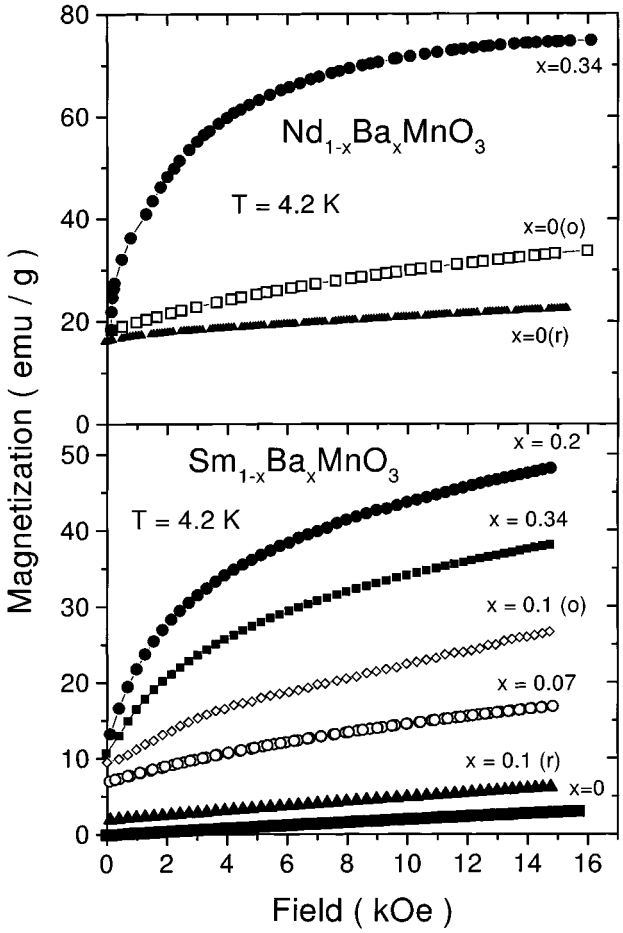

Figure 2. Magnetization as a function of magnetic field for $Nd_{1-x}Ba_xMnO_3$ (o—$NdMnO_{3.03}$, r—$NdMnO_{2.99}$) and $Sm_{1-x}Ba_xMnO_3$ (o—$Sm_{0.9}Ba_{0.1}MnO_{3.01}$, r—$Sm_{0.9}Ba_{0.1}MnO_{2.98}$) after cooling in a field of 14 kOe.

ionic sizes of different ions. The increase of the barium content leads to the gradual decrease of the orthorhombic crystal structure distortions. In view of the small magnitude of these distortions we did not manage to account precisely for the unit cell parameters for the $x > 0.2$ samples. Herein pseudocubic parameters are presented. Both oxidized and reduced samples of $Nd_{1-x}Ba_xMnO_{3-y}$ ($x > 0.2$; $y < 0.25$) composition were indexed in the pseudocubic perovskite structure. The volume of unit cell increases markedly with increase of the oxygen vacancies content probably due to conversion of small Mn^{4+} ions into large Mn^{3+} ions. The samarium-based samples exhibit larger unit cell distortions in comparison with the Nd series. However above $x = 0.3$ the crystal structure distortions for the samples prepared in air become very small similarly to the Nd-based series.

Magnetization data for $NdMnO_{3.03}$ and $SmMnO_{3.01}$ on heating in a field of 0.26 kOe after cooling in a field of 11 kOe are shown in figure 1 as a function of temperature. After cooling in a field of 11 kOe magnetic moments of all the magnetic domains align parallel to an external magnetic field. After removing the magnetic field this magnetic state does not decay due to large magnetic anisotropy. The large magnetic anisotropy is associated with

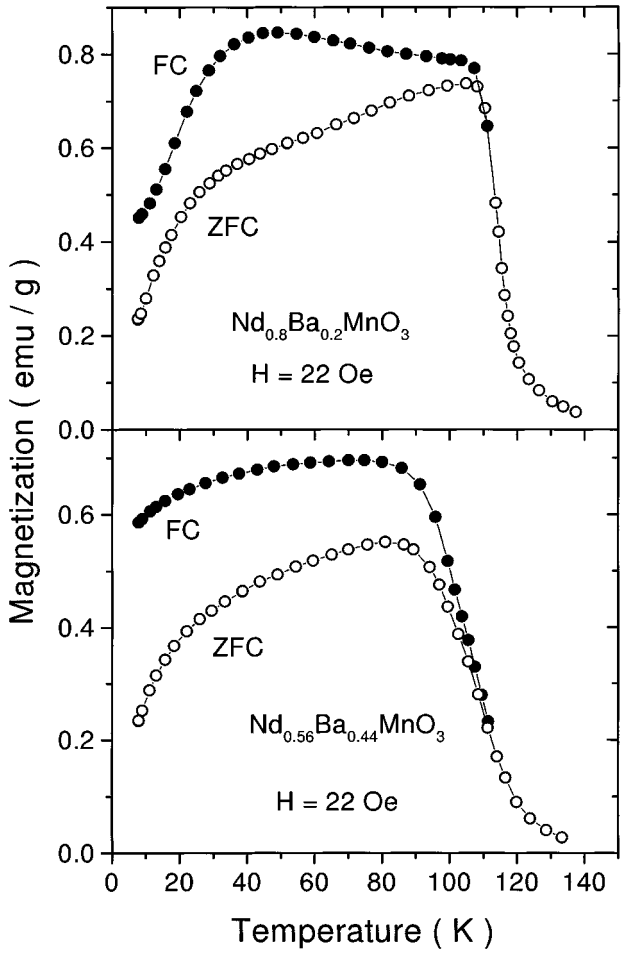

Figure 3. Magnetization as a function of temperature for $Nd_{1-x}Ba_xMnO_3$ in a low field regime.

manganese ions because it is known that $EuMnO_{2.99}$ (there is no magnetic contribution from the Eu^{3+} ion) shows a coercive field around 20 kOe at 4.2 K [8]. The magnetic ordering in $NdMnO_{3.03}$ and $SmMnO_{3.01}$ occurs at around 87 K and 57 K respectively where spontaneous magnetization appears. The anomalous magnetization behaviour arises apparently from the rare-earth sublattice magnetic contribution. In both cases the rare-earth magnetic moments are aligned opposite to the manganese ones; however for the Nd-based manganites f–d exchange coupling seems to be stronger because the anomalous behaviour is observed at relatively high temperature nearly the Néel point. The negative magnetization in a relatively small positive magnetic field arises from the large magnetic anisotropy associated with strongly distorted $Mn^{3+}O_6$ octahedra. The spontaneous ferromagnetic moment could be attributed to an interaction of Dzyaloshynsky–Morya type [7]. Suggesting that the magnetic moment due to manganese sublattice ordering in $NdMnO_3$ and $SmMnO_3$ is similar to that in $LnMnO_3$ and $EuMnO_3$ where the lanthanide is a nonmagnetic ion we can estimate the magnetic contribution for Nd^{3+} and Sm^{3+} ions. For $NdMnO_{2.99}$ the total magnetic moment at 5 K is $\approx 0.86\ \mu_B$ fu^{-1}. Hence the magnetic moment from the Nd sublattice is $\approx 0.8\ \mu_B$ fu^{-1} supposing that the magnetic moment per manganese ion is $\approx 0.06\ \mu_B$ fu^{-1} as observed for $LaMnO_3$ and $EuMnO_3$

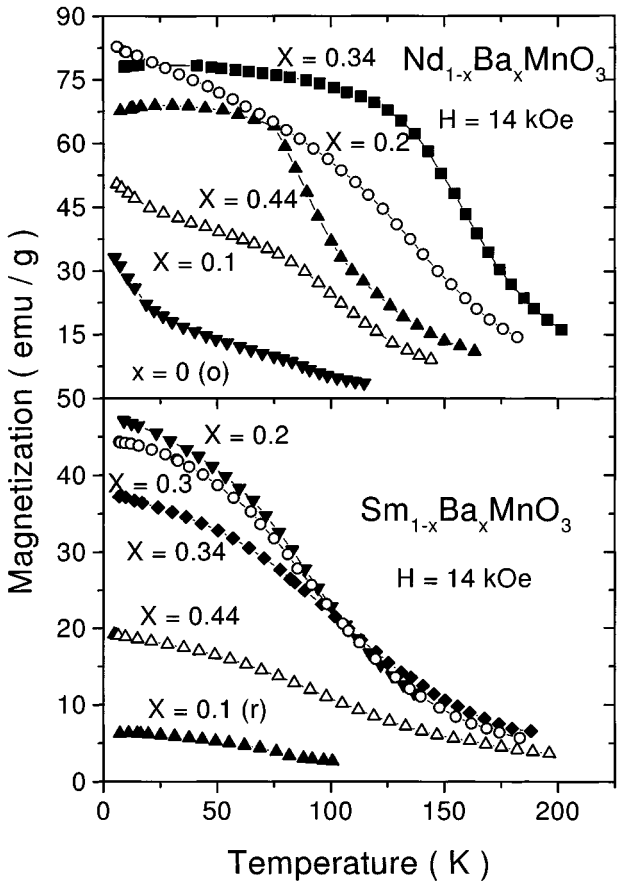

Figure 4. Magnetization as a function of temperature for the $Nd_{1-x}Ba_xMnO_3$ and $Sm_{1-x}Ba_xMnO_3$ series registered in a field of 14 kOe.

[8]. For $SmMnO_{3.01}$ the total magnetic moment is 0.0 μ_B fu^{-1} at 5 K. Therefore the samarium contribution compensates the manganese magnetic moment.

The substitution of Nd with Ba ions brought about the enhancement of both the magnetization and temperature of magnetic ordering (figures 2–4). The $Nd_{0.66}Ba_{0.34}MnO_3$ sample shows the largest Curie point 146 K. It is difficult to estimate the rare-earth contribution for the samples containing Mn^{4+} ions because the manganese contribution is unknown. However the field cooled magnetization for samples with large Ba content ($x \geqslant 0.2$) decreases strongly at low temperature thus indicating opposite alignment of magnetic moments of Mn and Nd sublattices (figure 3). Hence, the neodymium sublattice reduces the total magnetic moment. The magnetic moment due to parallel alignment of Mn^{3+} and Mn^{4+} magnetic moments (4 and 3 μ_B respectively) should be slightly below 4 μ_B per unit cell. The magnetic moment of $Nd_{0.8}Ba_{0.2}MnO_3$ at 4.2 K is 3.4 μ_B which indicates a pure ferromagnetic state owing to ordering of magnetic moments in a manganese sublattice. The decrease of both the magnetization and the Curie point is observed for the $x > 0.4$ compositions. The magnetization data for the single crystal of $Nd_{0.77}Ba_{0.23}MnO_3$ composition resemble those for the $Nd_{0.8}Ba_{0.2}MnO_3$ ceramics (figures 4 and 5). The ferromagnetic ordering in the single crystal occurs in the temperature interval 127–133 K. The temperature hysteresis ($\sim$3 K) is in agreement with first order magnetic phase transition, however this transition in a large magnetic field is relatively smooth (figure 5).

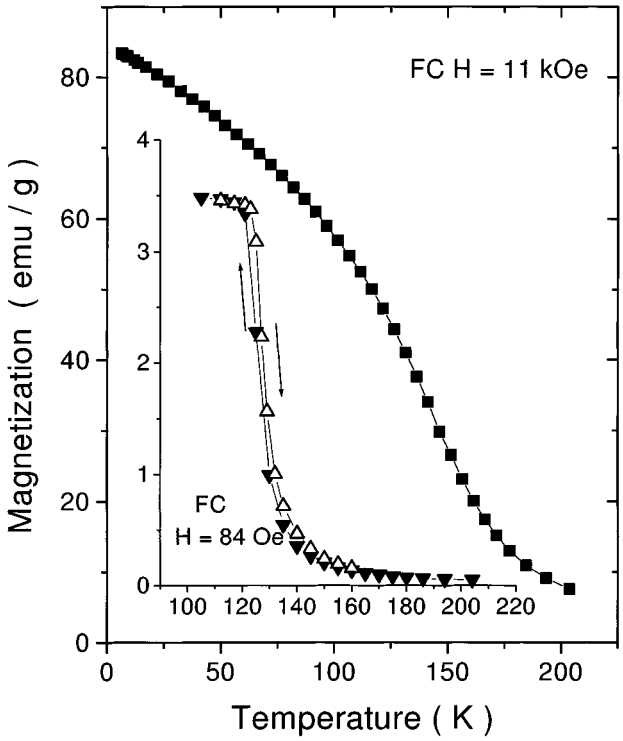

Figure 5. Magnetization as a function of temperature for the $Nd_{0.77}Ba_{0.23}MnO_3$ single crystal. The inset shows FC dependences on cooling and on heating in a field of 84 Oe.

$Sm_{1-x}Ba_xMnO_3$ ($x = 0.07$; 0.10; 0.12) oxidized samples exhibit a relatively sharp transition in the magnetically ordered state at around 60 K (figure 6). Spontaneous magnetization of these compounds is slightly more than that of the parent $SmMnO_3$ compound whereas the transition into the paramagnetic state is less pronounced thus indicating an inhomogeneous antiferromagnetic (antiferromagnetic matrix + ferromagnetic clusters) state. Reduction of $Sm_{0.9}Ba_{0.1}MnO_3$ nominal composition in the vacuum leads to an increase of Néel point up to 70 K; however spontaneous magnetization decreases markedly (figures 2, 6). These data are in agreement with the inhomogeneous state of lightly doped Sm-based manganites. Among the Sm-based samples the composition $x = 0.2$ exhibits the most pronounced ferromagnetic properties (figure 2). However, even in this case the relatively low spontaneous magnetic moment around 1.4 μ_B per formula unit is incompatible with the ferromagnetic state. The further increase of the Ba content leads to a decrease of the magnetization whereas the onset of the spontaneous magnetization appearance remains approximately the same as for the $x = 0.2$ composition. We have not observed any evidence of a long range ferromagnetic order for the samples $0.15 < x < 0.44$ by means of the low field magnetization measurements (figure 6). ZFC magnetization measured for the $x = 0.2$ sample shows a broad maximum around $T_r = 45$ K. Below this temperature the magnetic moments of ferromagnetic clusters are blocked with decreasing temperature.

The resistivity as a function of temperature for $Nd_{1-x}Ba_xMnO_3$ is presented in figure 7 (upper panel). The compositions with $0 < x < 0.3$ show an insulating behaviour in the whole investigated range of temperature $77 \leqslant T < 300$ K. The single crystal $x = 0.23$ exhibits an

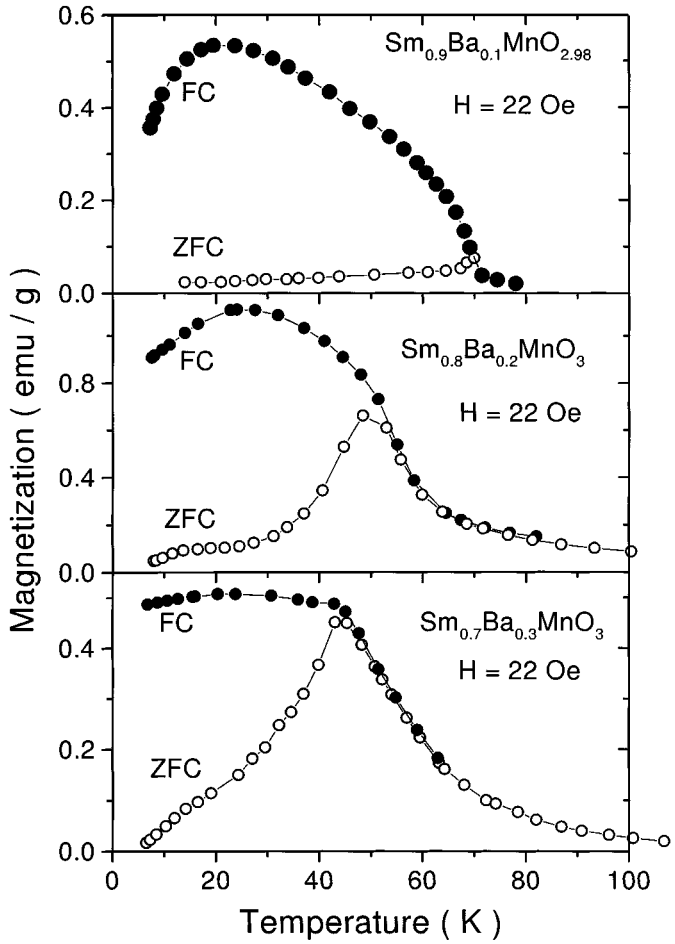

Figure 6. Magnetization behaviour of $Sm_{1-x}Ba_xMnO_3$ series in a low field regime.

anomaly at around T_C; however there is no transition into the metallic state. All the samples with the Ba content above $x = 0.3$ show metal–insulator transitions slightly below their Curie points. However the resistivity in the low temperature phase is relatively high, being incompatible with the true metallic state. All the ferromagnetic samples (both ceramics and single crystals, insulators as well as pseudometals) show similar temperature dependences of the magnetoresistance (figure 7, lower panel). For all the ferromagnetic samples the negative magnetoresistance defined as $\{[R(H = 9\ \text{kOe}) - R(H = 0)]/R(H = 0)\} \times 100\%$ reaches 40–70% around the Curie point. In contrast with the Nd(Ca, Sr)MnO_3 compounds [9] the Ba doped ones do not show metamagnetic behaviour or an irreversibility in the resistivity after application of a magnetic field. There is no transition into the metal-like state for the Sm-based compounds. The resistivity for these compounds decreases gradually with increasing Ba concentration, however remains very large (10^5–10^6 Ω cm at 77 K) even for $x = 0.44$.

The resistivity behaviour as a function of magnetic field value for the single crystal is shown in figure 8. The magnetoresistance in a large magnetic field of 120 kOe depends slightly on temperature both below and above the Curie point over the temperature range $100 < T < 150$ K. Below the Curie point the most pronounced changes occur in relatively

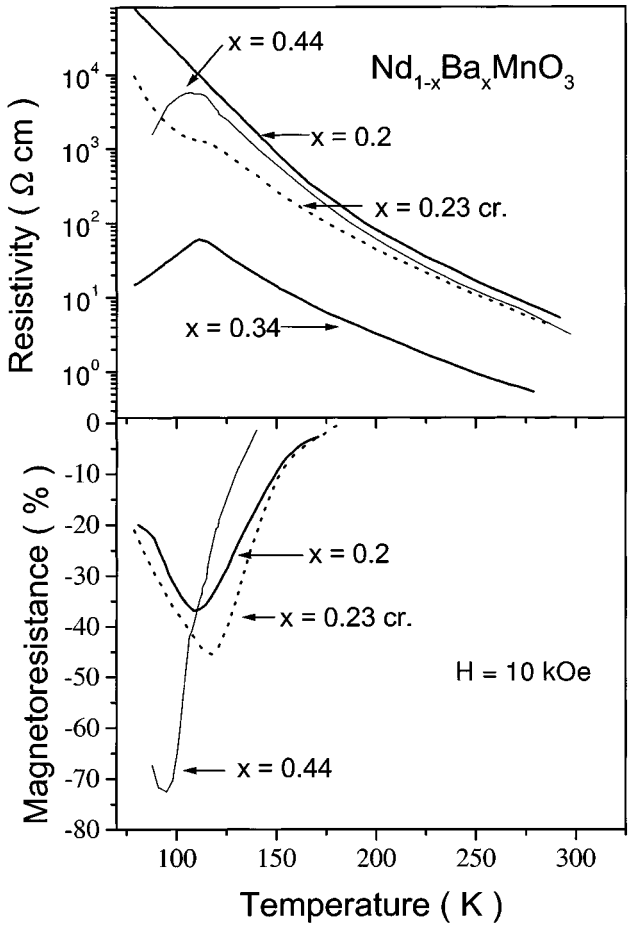

Figure 7. Resistivity and magnetoresistance as a function of temperature for the $Nd_{1-x}Ba_xMnO_3$ series.

small fields whereas above the Curie point the magnetoresistance increases strongly in a large magnetic field regime.

The magnetic phase diagrams for $Nd_{1-x}Ba_xMnO_3$ and $Sm_{1-x}Ba_xMnO_3$ are shown in figure 9. The $NdMnO_3$ and $SmMnO_3$ parent compounds are weak ferromagnets with $T_N = 87$ K and $T_N = 57$ K respectively. The substitution of rare earth with barium creates the ferromagnetic clusters or a noncollinear magnetic structure as predicted by the double exchange model [10]. The results of the magnetization studies in a low magnetic field [11], NMR [12] and neutron diffraction in a magnetic field [13] support the first point of view. We think that the ferromagnetism at first arises in the domains enriched by Mn^{4+} ions where the cooperative Jahn–Teller distortions are removed. According to Goodenough's consideration of exchange interactions in the system of mixed valence manganese ions in the perovskite lattice the Mn^{3+}–O–Mn^{3+} and Mn^{3+}–O–Mn^{4+} exchange interactions become ferromagnetic when the static Jahn–Teller distortions are removed [7]. The results of the study of manganites without Mn^{4+} ions in the orbitally disordered phases [14] are in agreement with this assumption. In the Nd-based series cooperative Jahn–Teller distortions are removed at $x \approx 0.1$ (table 1). The Sm-based manganites are more distorted due to a large mismatch between Sm and Mn ionic radii

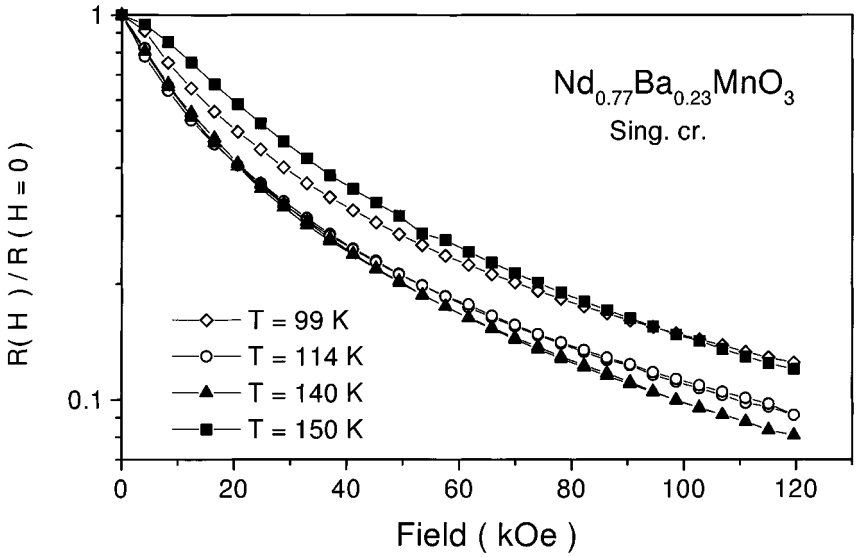

Figure 8. Magnetoresistance ratio as a function of magnetic field for the $Nd_{0.77}Ba_{0.23}MnO_3$ single crystal.

Table 1. Crystal structure parameters (a, b, c, V) and symmetry (O′—orthorhombic, O—orthorhombic, C—pseudocubic) for selected samples.

Composition	Sym.	a (Å)	b (Å)	c (Å)	V (Å^3)
$NdMnO_{3.03}$	O′	5.414	5.829	7.551	59.57
$Nd_{0.92}Ba_{0.08}MnO_3$	O′	5.451	5.689	7.634	59.18
$Nd_{0.9}Ba_{0.1}MnO_3$	O′	5.459	5.656	7.658	59.11
$Nd_{0.88}Ba_{0.12}MnO_3$	O	5.431	5.624	7.734	59.06
$Nd_{0.8}Ba_{0.2}MnO_3$	C	3.891			58.89
$Nd_{0.77}Ba_{0.23}MnO_3$	C	3.889			58.87
$Nd_{0.66}Ba_{0.34}MnO_3$	C	3.883			58.55
$Nd_{0.56}Ba_{0.44}MnO_3$	C	3.891			58.89
$Nd_{0.56}Ba_{0.44}MnO_{2.85}$	C	3.914			59.99
$SmMnO_{3.01}$	O′	5.371	5.831	7.498	58.71
$Sm_{0.93}Ba_{0.07}MnO_3$	O′	5.392	5.787	7.523	58.69
$Sm_{0.9}Ba_{0.1}MnO_3$	O′	5.401	5.768	7.534	58.68
$Sm_{0.8}Ba_{0.2}MnO_3$	O	5.453	5.571	7.720	58.63
$Sm_{0.66}Ba_{0.34}MnO_3$	C	3.882			58.49
$Sm_{0.56}Ba_{0.44}MnO_3$	C	3.883			58.55
$Sm_{0.56}Ba_{0.44}MnO_{2.85}$	C	3.900			59.35

thus leading to a stabilization of the Jahn–Teller local distortions. The Goodenough–Kanamori rule predicted the superexchange interaction between d^4 (Mn^{3+}) and d^3 (Mn^{4+}) to be positive for $\theta = 180^\circ$ and negative for $\theta = 90^\circ$. Hence a large angular dependence of the interaction is naturally expected as a result of the opposite signs at these two limiting angles. The concurrence between negative and positive superexchange interactions leads to a spin glass state for the Sm-based series.

Another effect which must be taken into consideration is the 3d-bandwidth variation due to the mismatch between rare-earth and manganese sublattices. The substitution of rare-earth ions

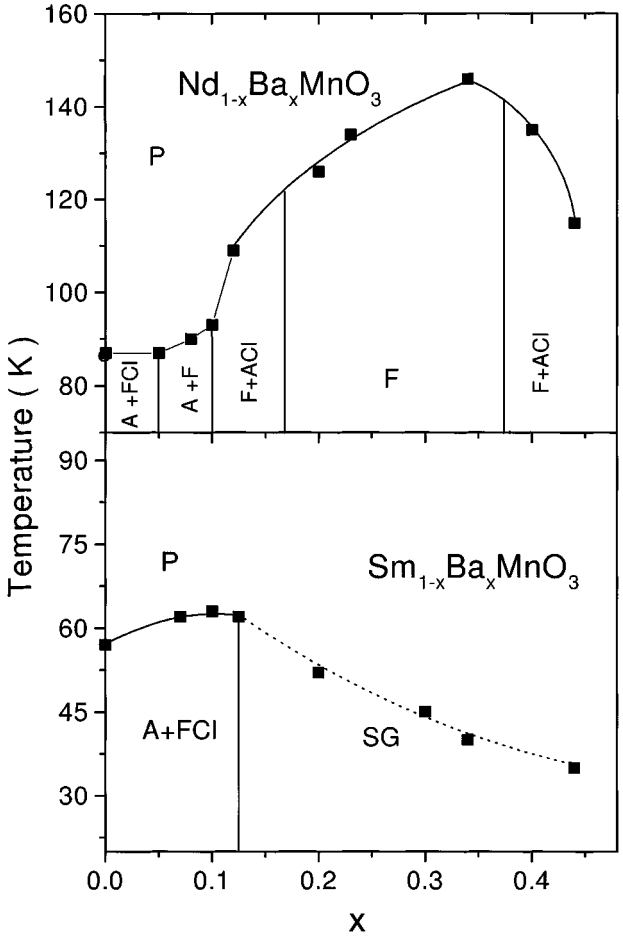

Figure 9. Magnetic phase diagrams for the $Nd_{1-x}Ba_xMnO_3$ and $Sm_{1-x}Ba_xMnO_3$ series. A—weak ferromagnet, F—ferromagnet, FCl—ferromagnetic clusters, ACl—antiferromagnetic clusters.

by barium leads to an increase of the 3d bandwidth because the crystal structure distortions are removed. Due to this effect both antiferromagnetic and ferromagnetic interactions should be increased. However the critical point for Nd-based manganites in the range $x \leqslant 0.10$ depends slightly on the composition apparently due to a concurrence between antiferromagnetic and ferromagnetic components within the O′-orthorhombic concentrational range. In the range $0.1 < x < 0.2$ where cooperative Jahn–Teller distortions are removed the Curie point increases strongly.

Above $x = 0.4$ a new antiferromagnetic state is developed. We think that this antiferromagnetic state is not connected with the charge ordering as observed in Nd(Ca, Sr)MnO_3 manganites [9] because there are no metamagnetic and irreversibility effects in the magnetization and resistivity behaviour. It is probable that at $x \geqslant 0.4$ the Mn^{3+}–O–Mn^{4+} positive superexchange decreases whereas the Mn^{4+}–O–Mn^{4+} negative superexchange increases thus leading to a stabilization of the A-type antiferromagnetic structure observed in the heavily doped (Ln, Sr)MnO_3 (Ln = La, Nd) manganites by means of the neutron diffraction method [15].

We suggest that electrical transport properties could be interpreted as follows. The Mn^{4+} ions introduced by a small quantity of Ba^{2+} remain tightly bound to all the nearest neighbour manganese ions and act as acceptor levels. As barium content increases, the acceptor complexes interact to form an impurity 3d-manganese band.

We think that exchange interaction between e_g charge carriers and t_{2g} localized electrons is comparable with the impurity 3d bandwidth. Therefore at T_C the effective impurity 3d bandwidth increases strongly due to the parallel alignment of charge carriers and t_{2g} electrons. The broadening of the impurity 3d bandwidth due to both the magnetic ordering and the replacement of Nd by Ba leads to decrease of the gap between the narrow impurity 3d band and wide 2p-oxygen band. Above $x = 0.15$ the pure ferromagnetic state is realized; however the 3d bandwidth is too small for the appearance of metal-like conductivity. Further increase of the Ba content leads to an increase of the 3d bandwidth due to increase of the Mn–O–Mn angle whereas doping induces a decrease in electron correlation energy. Therefore the gap between the wide 2p-oxygen band and impurity band decreases thus leading to a metal-like behaviour for $x \geqslant 0.3$ compositions. The observation of 2p oxygen hole driven conductivity in the manganites [16] is in favour of such a mechanism of metal–insulator transition in the manganites.

The magnetoresistance properties exhibited by ferromagnetic samples of the $Nd_{1-x}Ba_xMnO_3$ system are similar to those of the doped EuO [17], $Cd_2Cr_2Se_4$ [17] and $Tl_2Mn_2O_7$ [18] compounds. In all these systems magnetoresistance is negative and reaches 30–60% in a field of 10 kOe around the Curie point. The maximum of the resistivity occurs as a rule slightly below the Curie point. Apparently the huge magnetoresistance in all these systems may be the result of a decreasing gap between the impurity levels and wide conduction band due to application of an external magnetic field. In this model the maximal effect is realized near the concentrational metal–insulator transition.

Acknowledgment

This work was supported in part by the Belarus Fund for Fundamental Research (grant F98-056) and NATO grant No PST-CLG-975703.

References

[1] Barnabe A, Millange F, Maignan A, Hervieu M and Raveau M 1998 *Chem. Mater.* **10** 252
[2] Troyanchuk I O, Kolesova I M, Szymczak H and Nabialek A 1997 *J. Magn. Magn. Mater.* **176** 267
[3] Ju H L and Sohn H 1997 *Solid State Commun.* **102** 463
[4] Maignan A, Martin C, Hervieu M, Raveau B and Hejtmanek J 1998 *Solid State Commun.* **107** 363
[5] Damay F, Nguyen N, Maignan A, Herveu M and Raveau B 1996 *Solid State Commun.* **98** 11 997
[6] Rodrigez-Martinez L M and Attfield J P 1996 *Phys. Rev.* B **54** R15 622
[7] Goodenough J B 1963 *Magnetism and the Chemical Bond* (New York: Wiley)
[8] Troyanchuk I O, Samsonenko N V, Kasper N V, Szmyczak H and Nabialek A 1997 *J. Phys.: Condens. Matter* **9** 9297
[9] Kuwahara H, Tomioka Y, Asamitsu A, Moritomo Y, Kumai R, Kasai M and Tokura Y 1996 *Science* **272** 80
[10] De Gennes P 1960 *Phys. Rev.* **118** 141
[11] Troyanchuk I O 1992 *Sov. Phys.–JETP* **75** 132
[12] Allodi G, De Renzi R, Guidi G, Licci F and Pieper M W 1997 *Phys. Rev.* B **56** 6036
[13] Wollan E O and Koehler W C 1955 *Phys. Rev.* **100** 545
[14] Troyanchuk I O, Khalyavin D D, Shapovalova E F, Kasper N V and Guretskii S A 1998 *Phys. Rev.* B **58** 2422
[15] Moritomo Y, Akimoto T, Nakamura A, Ohoyama R and Ohashi M 1998 *Phys. Rev.* B **58** 5544
[16] Ju H L, Sohn H-C and Krishnan K M 1997 *Phys. Rev. Lett.* **79** 3230
[17] Methfessel S and Mattis D C 1968 *Magnetic Semiconductors (Handbuch der Physik XYIII/1)* (Berlin: Springer)
[18] Kwei G H, Booth C H, Bridges F and Subranmanian M A 1997 *Phys. Rev.* B **55** R68